AGU PUBLICATIONS

Geophysical Research Letters

RESEARCH LETTER
10.1002/2015GL064609

Key Points:
- Aircraft observation-based hurricane wind climatology is created
- Evaluation of hurricane intensity predictions beyond simplistic point metrics
- Ensemble forecast loses predictive skill during rapid intensification

Correspondence to:
F. Judt,
fjudt@rsmas.miami.edu

Citation:
Judt, F., and S. S. Chen (2015), A new aircraft hurricane wind climatology and applications in assessing the predictive skill of tropical cyclone intensity using high-resolution ensemble forecasts, *Geophys. Res. Lett.*, *42*, 6043–6050, doi:10.1002/2015GL064609.

Received 18 MAY 2015
Accepted 9 JUN 2015
Accepted article online 12 JUN 2015
Published online 16 JUL 2015
Corrected 18 AUG 2015

This article was corrected on 18 AUG 2015. See the end of the full text for details.

A new aircraft hurricane wind climatology and applications in assessing the predictive skill of tropical cyclone intensity using high-resolution ensemble forecasts

Falko Judt[1] and Shuyi S. Chen[1]

[1]Rosenstiel School of Marine and Atmospheric Science, University of Miami, Miami, Florida, USA

Abstract Hurricane surface wind is a key measure of storm intensity. However, a climatology of hurricane winds is lacking to date, largely because hurricanes are relatively rare events and difficult to observe over the open ocean. Here we present a new hurricane wind climatology based on objective surface wind analyses, which are derived from Stepped Frequency Microwave Radiometer measurements acquired by NOAA WP-3D and U.S. Air Force WC-130J hurricane hunter aircraft. The wind data were collected during 72 aircraft reconnaissance missions into 21 western Atlantic hurricanes from 1998 to 2012. This climatology provides an opportunity to validate hurricane intensity forecasts beyond the simplistic maximum wind speed metric and allows evaluating the predictive skill of probabilistic hurricane intensity forecasts using high-resolution model ensembles. An example of application is presented here using a 1.3 km grid spacing Weather Research and Forecasting model ensemble forecast of Hurricane Earl (2010).

1. Introduction

Hurricane intensity is traditionally defined by the maximum surface wind speed anywhere within the storm [*Landsea and Franklin*, 2013], and numerical model predictions of hurricane intensity are commonly evaluated with National Hurricane Center (NHC) "best track" intensity estimates. However, quantitative evaluations of probabilistic hurricane intensity predictions by numerical model ensembles have been almost nonexistent, largely due to the lack of real observational data and suitable long-term statistics.

Climatologies of meteorological variables such as winds can be used to evaluate the predictive skill of weather and climate model ensemble predictions [*Schneider and Griffies*, 1999; *Kleeman*, 2002; *Komaromi and Majumdar*, 2014]. Predictive skill is examined by comparing the forecasted frequency distribution of a variable (i.e., the predicted uncertainty) to the climatological distribution of the same variable, which represents a distribution of all historical outcomes (i.e., the climatological uncertainty). The prediction is said to be skillful when the forecast distribution differs from the climatological distribution (Figure 1), and predictive skill is lost once the forecast frequency distribution cannot be distinguished from the climatological distribution [*Schneider and Griffies*, 1999; *Cai et al.*, 2002; *Kleeman*, 2002; *DelSole*, 2004; *DelSole and Tippett*, 2007; *Giannakis and Majda*, 2012].

So far, this method has not been used to evaluate the predictive skill of hurricane intensity predictions in high-resolution prediction ensembles. One reason is the lack of an appropriate hurricane wind climatology, since hurricanes are relatively rare events and wind observations limited. This paper describes the development of a novel wind speed climatology based on surface wind analyses, which were derived from aircraft measurements in 21 Atlantic hurricanes from 1998 to 2012. We then use the climatology to investigate the predictive skill of wind forecasts in a high-resolution forecast ensemble of Hurricane Earl (2010).

In a recent study, *Komaromi and Majumdar* [2014] used climatological distributions of various quantities from global model reanalysis fields to investigate the predictability of tropical cyclogenesis. However, reanalysis products are constrained by model resolution, limited observations, and other potential shortcomings. *Schenkel and Hart* [2012] showed that the representation of hurricane intensity in reanalysis products is problematic. Furthermore, reanalyses do not constitute a "true" climatology based on historical observations, and reanalysis climatologies may be biased [*Giannakis and Majda*, 2012]. These issues make it imperative to use a climatology based on observations when investigating the predictive skill of hurricane intensity forecasts. *Uhlhorn et al.* [2014] presented an observation-based climatology of Atlantic hurricane winds to investigate storm asymmetries. This paper introduces a much more detailed climatology

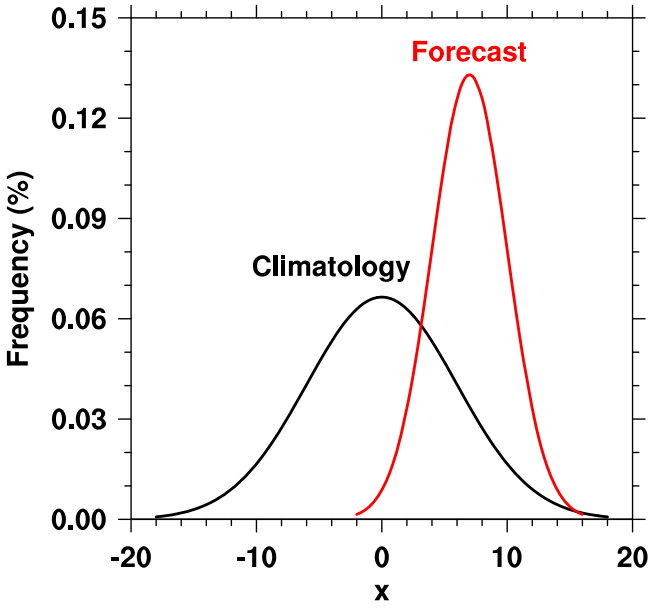

Figure 1. Schematic of climatological and forecast frequency distributions. The difference between the distributions determines the predictive skill (adapted from *DelSole and Tippett* [2007]).

of the wind distribution in hurricanes and demonstrates for the first time how a probabilistic hurricane wind climatology can be used to validate forecast ensembles beyond the simplistic maximum wind speed metric.

2. An Aircraft Observation-Based Hurricane Wind Climatology

The wind field analyses used for this climatology are derived from airborne Stepped Frequency Microwave Radiometer (SFMR) surface wind speed measurements. SFMR instruments are mounted under the wings of "hurricane hunter" aircraft and use microwave radiation emitted from the ocean surface to estimate the surface wind speed [*Delnore et al.*, 1984; *Uhlhorn and Black*, 2003; *Uhlhorn et al.*, 2007; *Klotz and Uhlhorn*, 2014]. The first well-calibrated SFMR measurements were made on NOAA research flights in 1998, and since 2007, all U.S. Air Force and NOAA hurricane hunter aircraft are equipped with SFMRs.

Here we create a wind climatology of hurricanes that recurve over the western Atlantic Ocean, away from land. The climatology is composed of 72 wind field analyses from 21 hurricanes that occurred between 1998 and 2012. Storm tracks and flight paths of the 72 aircraft missions are shown in Figure 2, along with a list of the hurricanes and the number of aircraft missions into each storm.

The hurricane wind climatology was constructed in a storm-relative framework. Objective analyses of the hurricane surface wind fields were obtained by a semispectral procedure, which retrieved the wave

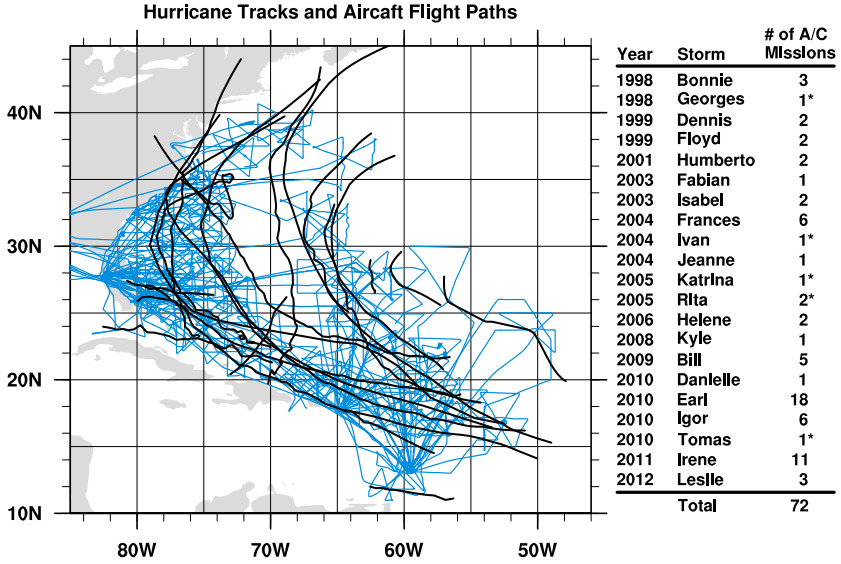

Year	Storm	# of A/C Missions
1998	Bonnie	3
1998	Georges	1*
1999	Dennis	2
1999	Floyd	2
2001	Humberto	2
2003	Fabian	1
2003	Isabel	2
2004	Frances	6
2004	Ivan	1*
2004	Jeanne	1
2005	Katrina	1*
2005	Rita	2*
2006	Helene	2
2008	Kyle	1
2009	Bill	5
2010	Danielle	1
2010	Earl	18
2010	Igor	6
2010	Tomas	1*
2011	Irene	11
2012	Leslie	3
	Total	72

Figure 2. Tracks of the 21 Atlantic hurricanes from 1998 to 2012 (black lines) that were used for the wind climatology, overlaid with flight paths of the 72 aircraft missions (blue lines). The 21 hurricanes with the respective number of aircraft missions into each storm are listed on the right. For hurricanes denoted with an asterisk (*), only the missions that took place before the storms entered the Gulf of Mexico or the Caribbean Sea were used.

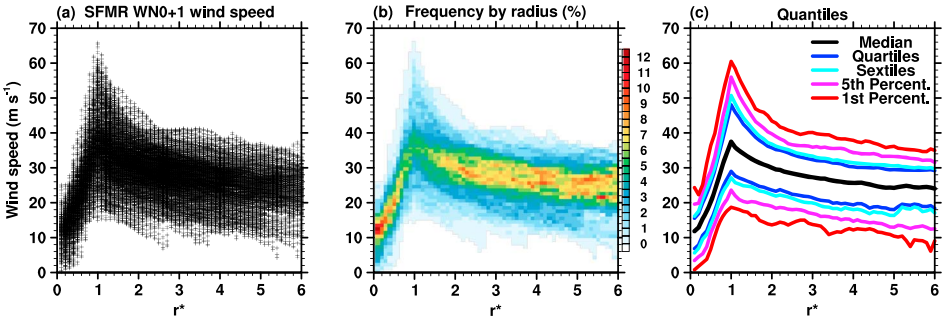

Figure 3. (a) Surface wind speed from the climatology as a function of normalized distance from storm center (r^*). (b) Wind speed frequency by radius distribution based on the data in Figure 3a. (c) Selected upper and lower quantiles (median, quartiles, sextiles, 5th percentiles, and 1st percentiles) from the distribution in Figure 3b.

number (WN) 0 and 1 components of the wind field from the SFMR measurements [*Uhlhorn et al.*, 2014]. All 72 WN 0 + 1 wind field analyses were interpolated onto a common polar grid (radius r, azimuth θ). To isolate changes in intensity from wind field expansions or contractions, the radial distance from the storm center was normalized by the radius of maximum wind (RMW, r_{max}) so that the climatology is represented in the normalized radius coordinate r^*, where $r^* = r/r_{max}$.

The wind climatology (radial distribution of surface wind speed) is shown in Figure 3a. The overall shape of the wind speed distribution shows the typical radial wind structure of hurricanes: the strongest winds are found near the eyewall ($r^* = 1$), wind speed decreases abruptly inside the RMW ($r^* < 1$) as one enters the hurricane eye, and it decreases more gradually radially outward in the inner core ($r^* = 1$–2) and rainband region ($r^* = 2$–6).

To produce a probabilistic wind distribution, the data points shown in Figure 3a were binned to compute the frequency of wind speed occurrence as a function of normalized radius (bin widths: $\Delta r^* = 0.1$ and $\Delta v = 1\ \mathrm{m\ s^{-1}}$). The result is a "wind speed frequency by radius" distribution (Figure 3b), where a "slice" at any given r^* can be interpreted as a one-dimensional frequency distribution of wind speed at that particular radius. The wind speed frequency distribution can be converted into a "contoured frequency by radius diagram," which highlights selected quantiles of the underlying frequency distribution (Figure 3c). It has a similar meaning as the "contoured frequency by altitude diagrams" shown by *Yuter and Houze* [1995]. Figure 3c displays the median, quartiles, sextiles, and the upper and lower 1st and 5th percentiles. The distribution is widest in the eyewall region, where the interquartile range (difference between upper and lower quartiles) is 19.1 m s^{-1}. Radially outward, little difference in terms of distribution width is found between the inner core and the rainband region, where the interquartile range is 12.1 m s^{-1} ($r^* = 2$) and 11.5 m s^{-1} ($r^* = 5$), respectively.

3. High-Resolution Forecast Ensemble of Hurricane Earl (2010)

The hurricane wind climatology can be used for assessing the predictive skill of numerical weather prediction model ensemble forecasts of hurricane intensity and perhaps future projections of hurricane intensity in climate models. Here we provide an example to demonstrate the use of the wind climatology for evaluating the predictive skill of hurricane intensity in a 100-member Weather Research and Forecasting (WRF) model ensemble of Hurricane Earl (2010). The ensemble was initialized with initial and lateral boundary conditions from the 0000 UTC 27 August 2010 Global Forecast System deterministic forecast and integrated for 7 days. A triply nested model configuration with two vortex-following domains (grid spacings of 12, 4, and 1.3 km, respectively) was used [*Davis et al.*, 2008]. The 7 day forecast period encompasses Earl's intensification from tropical storm to major hurricane, including a period of rapid intensification (RI), and the beginning of its extratropical transition. Ensemble variability was created by stochastically perturbing the u, v, and θ tendency equations with a stochastic kinetic energy backscatter scheme [*Shutts*, 2005; *Berner et al.*, 2009, 2011]. The ensemble method and forecasts are described in more detail in *Judt et al.* [2015].

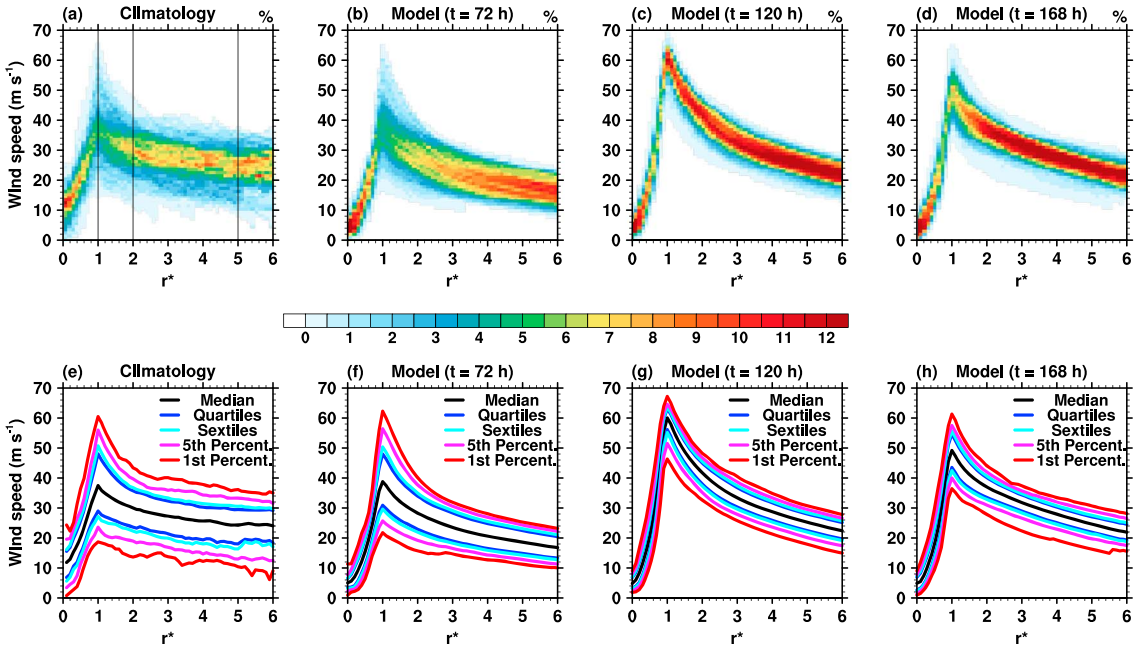

Figure 4. (a) Same as Figure 3b. (b–d) Wind speed frequency by radius distribution from the high-resolution forecast ensemble of Hurricane Earl (2010). Frequency distribution at $t = 72$ h (Figure 4b), frequency distribution at $t = 120$ h (Figure 4c), and frequency distribution at $t = 168$ h (Figure 4d). (e) Same as Figure 3c. (f–h) Selected quantiles based on the wind speed frequency distributions in Figures 4b–4d. Black lines in Figure 4a indicate the radii ($r^* = 1$, 2, and 5) of the frequency distributions shown in Figure 5.

To compare the wind speed frequency distributions from the ensemble forecast with the climatology, the surface wind speed fields of the ensemble hurricanes were converted to an analogous polar coordinate system, where the radial distance from the storm center was normalized by the RMW. To be consistent with the climatology, we only used the WN 0 and 1 components of the hurricane surface wind field. The WN 0 + 1 wind speed fields from the ensemble were then binned similarly to the SFMR wind analyses ($\Delta r^* = 0.1$, $\Delta\theta = 1.0°$, and $\Delta v = 1\ \mathrm{m\ s^{-1}}$).

4. Predictive Skill of Hurricane Intensity Forecasts

The WRF model control and ensemble forecasts of Hurricane Earl (2010) have been compared with the NHC best track data in terms of storm location and maximum wind in *Judt and Chen* [2014] and *Judt et al.* [2015]. The model forecasts captured the storm track and Earl's intensity evolution from a weak tropical storm to a category 4 hurricane over the 7 day period. However, the wind distribution over the entire storm, which is important for hurricane impact forecasting, cannot be evaluated with the best track data. Here we use the observed hurricane wind climatology to assess two main characteristics of the high-resolution ensemble forecasts: the hurricane wind field (WN 0 + 1) and wind speed distributions at specific radial locations.

First, we evaluate the predictive skill of the *vortex-scale* wind field, which represents the overall storm circulation, at three different times ($t = 72$ h, 120 h, and 168 h, Figures 4b–4d). The forecast distributions are characterized by a higher kurtosis compared to the climatological distribution, which implies that the forecast distributions are generally narrower and forecast uncertainty is less than the climatological wind uncertainty. Therefore, the ensemble provides more "useful" information than the climatology and has predictive skill. This result is consistent with the finding that the WN 0 + 1 component of the hurricane wind field remains predictable for > 7 days in long-lasting nonlandfalling hurricanes *Judt et al.* [2015].

While Figures 4b–4d provide a general view of the wind speed frequency distribution, the "contoured wind speed frequency by radius distribution" in Figures 4e–4h highlights selected quantiles and provides a more quantitative measure of uncertainty. The largest uncertainty in Hurricane Earl is during the RI period around

$t = 72$ h [*Judt and Chen*, 2014]. At $t = 72$ h, the width of the forecast distribution peaks in the eyewall region ($r^* = 1$), and the quantiles are spaced apart farther than at any other time during the forecast (Figure 4f). The wind speed range at $r^* = 1$ is 47.2 m s^{-1} (17.9 m s$^{-1} \leq v \leq$ 65.1 m s^{-1}), similar to the climatology's range of 51.1 m s^{-1} (14.7 m s$^{-1} \leq v \leq$ 65.9 m s^{-1}). The broad distribution at $t = 72$ h is a manifestation of the uncertainty in RI timing exhibited by the ensemble, as some ensemble storms are already mature hurricanes while others have not begun the RI process [*Judt and Chen*, 2014]. The range between the lower and upper 1st percentiles at $r^* = 1$, representing 98% of all wind speed values, is 40.5 m s^{-1} (Figure 4f). This value is comparable to the "inter-1st-percentile range" of the climatology (Figure 4e), which is 41.8 m s^{-1}. The increased uncertainty in the eyewall indicates that during the highly uncertain RI period, most of the intensity uncertainty is associated with variability in this region. This is not surprising, since the peak wind is well correlated with the azimuthally averaged wind speed at the RMW [*Vukicevic et al.*, 2014].

Two days later, at $t = 120$ h, all members have eventually intensified and evolved into strong hurricanes. Consequently, the width of the forecast wind speed frequency distributions has decreased (Figures 4c and 4g). Note that the forecast not only features less uncertainty than the climatology, but the whole distribution is shifted to higher wind speed values, most noticeably radially inward of $r^* = 3$. If the frequency distributions are interpreted as probability distributions, the ensemble forecast indicates that the likelihood of Earl having stronger winds is much higher than the climatological reference, which was the case in reality. The frequency distribution's uncertainty in the eyewall decreases significantly at $t = 120$ h, demonstrated by the fact that the inter-1st-percentile range reduces by about 50% from 40.5 m s^{-1} to 20.9 m s^{-1} (Figure 4g).

Toward the end of the forecast period, uncertainty increases again and the forecast frequency distribution broadens slightly (Figures 4d and 4h). Since some ensemble members begin the extratropical transition process, the peaked mode associated with the well-defined eyewalls at $t = 120$ h decreases in amplitude by $t = 168$ h. Uncertainty in the inner core and the rainband region increases somewhat compared to the maximum intensity period at $t = 120$ h.

Next, we demonstrate how the hurricane wind climatology can be used to assess the predictive skill of probabilistic forecasts of hurricane intensity. We chose three different radii to examine the ensemble wind speed forecasts, representing (1) the RMW ($r^* = 1$), (2) the inner core outside of the RMW ($r^* = 2$), and (3) the rainband region ($r^* = 5$). The respective wind speed frequency distributions in Figure 5 are one-dimensional frequency distribution functions and can be thought of as "slices" from the distributions in Figure 4 (radial locations of these slices are marked by black lines in Figure 4a). Figure 5 shows the ensemble forecast wind speed frequency distributions at the three selected radii for various times representative of the entire life cycle of Hurricane Earl. The developing stage ($t = 36$ h) is shown in Figures 5a, 5e, and 5i, the RI period ($t = 72$ h) in Figures 5b, 5f, and 5j, the mature stage ($t = 120$ h) in Figures 5c, 5g, and 5k, and the weakening phase ($t = 168$ h) in Figures 5d, 5h, and 5l. The predictive skill is measured against the climatology by whether the model forecast can capture the evolution of Earl from a weak tropical storm to a major hurricane. A two-sided Kolmogorov-Smirnov hypothesis test provides information on the difference between the climatological and forecast distributions. Following commonly used conventions, p values of < 0.05 indicate that the differences between the distributions are statistically significant at the 95% confidence level (p values are plotted in the top right corner of each panel in Figure 5).

At $t = 36$ h, the forecast distribution at the RMW is narrower than the climatology and shifted to lower wind speeds (Figure 5a, $p < 0.01$). This is a manifestation of nearly all ensemble members predicting Earl to be a tropical storm with wind speeds around 20–30 m s^{-1} in the RMW region, which is much weaker than an "average" hurricane represented by the climatology. The same is true for the wind speed distributions at $r^* = 2$ (Figure 5e, $p = 0.01$) and $r^* = 5$ (Figure 5i, $p = 0.01$), because the wind fields of the ensemble storms are still not as well developed as those of most hurricanes, meaning that there is less chance of higher winds. The maximum wind speed, a single-point metric and the traditional measure of hurricane intensity, is near the mode of the wind distribution in Figure 5a. According to NHC's best track, Earl's estimated maximum wind speed was ~26 m s^{-1} at this time.

At $t = 72$ h (Figure 5b, $p = 0.72$), during the hurricane RI period, the ensemble has diversified substantially. Some members have intensified into major hurricanes, while other members remained at tropical storm intensity [*Judt and Chen*, 2014]. As a result, the forecast uncertainty has increased significantly, and the forecast and climatological wind speed distributions at the RMW are remarkably similar. The high p value

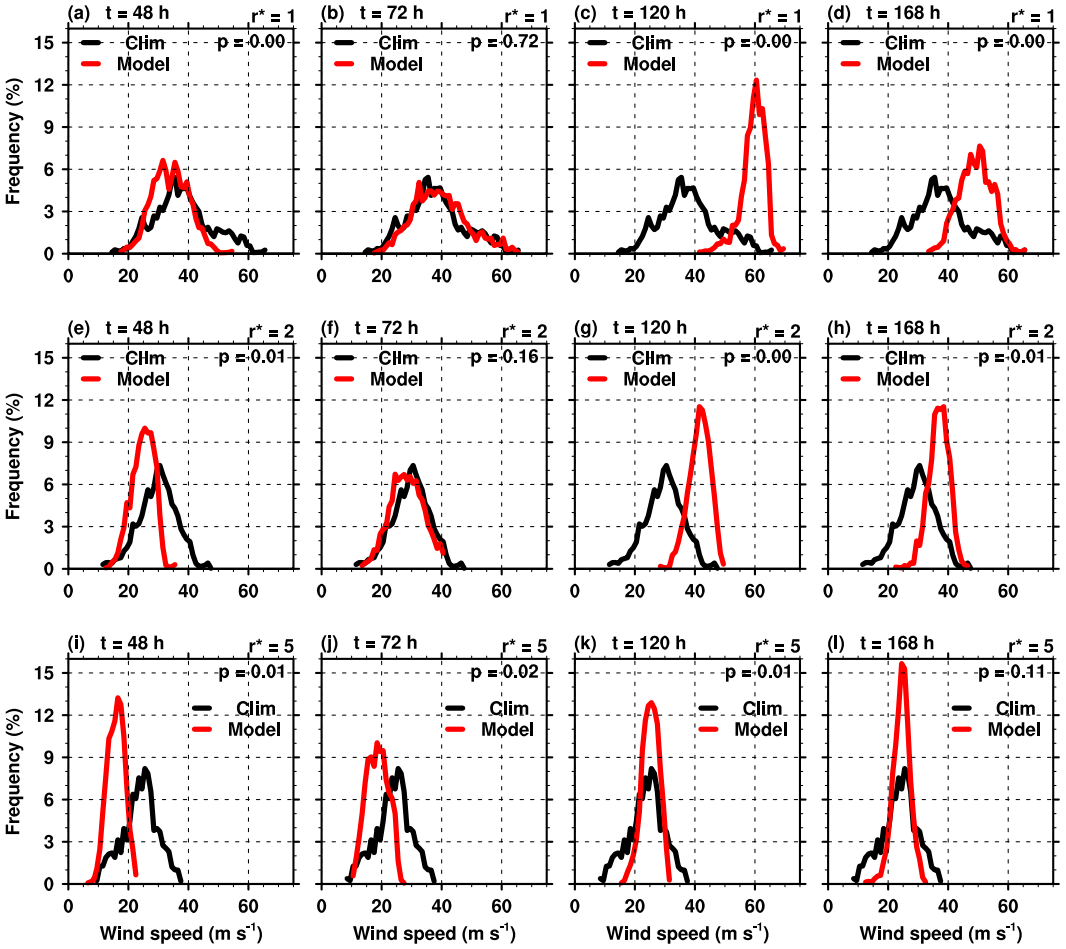

Figure 5. Wind speed frequency distributions at (a–d) $r^* = 1$, (e–h) $r^* = 2$, and (i–l) $r^* = 5$ at forecast times $t = 36$ h (Figures 5a, 5e, and 5i), $t = 72$ h (Figures 5b, 5f, and 5j), $t = 120$ h (Figures 5c, 5g, and 5k), and $t = 168$ h (Figures 5d, 5h, and 5l). The shown distributions can be interpreted as slices of the frequency by radius distributions in Figure 4 (radial locations marked by black lines in Figure 4a). Plotted in the top right corner of each panel are p values from a Kolmogorov-Smirnov hypothesis test, where $p < 0.05$ indicates that the differences between the distributions are statistically significant at the 95% confidence level.

of 0.72 indicates that the forecast and climatology in Figure 5b are practically indistinguishable, and the ensemble forecast has little skill compared with the climatology. Similarly at $r^* = 2$, the difference between the distributions is not statistically significant (Figure 5f, $p = 0.16$). At $r^* = 5$ (Figure 5j, $p = 0.02$), the forecast distribution indicates that wind speeds are likely to be weaker than climatology. This means that the ensemble forecasts of Hurricane Earl generally represent smaller storms or more compact outer wind fields than an average storm represented by the climatology.

By $t = 120$ h, *all* ensemble members have finally evolved into major hurricanes. Therefore, the mode of the RMW wind speed distribution has shifted to 60 m s^{-1} and the likelihood of high wind speeds has drastically increased, as shown by the substantial difference in the right tail of the distributions (Figure 5c, $p < 0.01$). According to the forecast, it is thus much more likely that Earl will be a very intense storm. For reference, Earl was indeed a major hurricane with maximum winds of 59 m s^{-1} at this time. In stark contrast to Figure 5b, the difference between the forecast and climatological distributions is now maximum. At $r^* = 2$, the forecast distribution has shifted to the right (Figure 5g, $p < 0.01$) compared to 2 days before, indicating that the inner core wind field has expanded. A similar shift has occurred in the outer region at $r^* = 5$ (Figure 5k, $p = 0.01$), showing that the wind field is generally growing. Note that the climatological distribution is narrower at $r^* = 2$ and $r^* = 5$ than at $r^* = 1$, and uncertainty differences

between the forecast and climatology are much less than at the RMW. This suggests that the wind speed at larger radii tends to be not as variable as in the eyewall, and the forecast cannot reduce the uncertainty as significantly.

By $t = 168$ h, the forecast distribution at the RMW has shifted to lower values, as the ensemble storms start to weaken and their RMW increases (Figure 5d, $p < 0.01$). This is consistent with the increased uncertainty of vortex structure during this period *Judt et al.* [2015], and extreme wind speeds near the RMW are increasingly unlikely. At $r^* = 2$ (Figure 5h, $p = 0.01$), the mode of the forecast is about $5\,\mathrm{m\,s^{-1}}$ higher than that of the climatology, a manifestation of the radially outward region of high winds. The elevated wind speed in this region is indicative of the typical broadening of the wind field that occurs during extratropical transition. At $r^* = 5$ (Figure 5l, $p = 0.11$), the distributions are fairly similar and the difference is not statistically significant, although the forecast distribution is somewhat narrower.

5. Summary and Conclusions

This study introduces a novel hurricane wind climatology based on aircraft observations. The comprehensive, storm-relative climatology of hurricane surface wind speed is composed of wind field analyses that were derived from SFMR measurements taken during 72 aircraft missions into 21 Atlantic hurricanes between 1998 and 2012. We demonstrate how the climatology can be used to validate prediction models beyond the simplistic verification of maximum wind speed, and we assess the predictive skill of hurricane wind speed forecasts in a high-resolution forecast ensemble of Hurricane Earl (2010).

The climatological wind speed frequency distribution is used to evaluate the predictive skill of an ensemble forecast from a high-resolution model by assessing whether the model provides more useful information than the climatology (i.e., less uncertainty). A storm-scale overview shows that the climatological distribution is generally broader than the forecast distribution. The ensemble is skillful at predicting the storm-scale wind speed field throughout the 7 day forecast. This finding is consistent with the predictability analysis of *Judt et al.* [2015], which showed that the wave number $0+1$ component of the hurricane wind field in Earl remains predictable for > 7 days.

A further evaluation of the probabilistic wind forecasts at various radii over time reveals that the forecast distributions became very similar to that of climatology when Hurricane Earl intensified rapidly. This result suggests that the predictive skill of an intensifying hurricane is relatively low or less predictable, which confirms what has been documented in *Judt and Chen* [2014].

The hurricane wind climatology offers new ways to assess the predictive skill of hurricane intensity compared to predictability analyses focusing on a particular metric such as the peak wind. Future studies may be able to perform quantitative calculations of metrics such as relative entropy or predictive power [*Schneider and Griffies*, 1999; *Kleeman*, 2002; *Komaromi and Majumdar*, 2014].

Acknowledgments

The SFMR surface wind analyses were kindly provided by Eric W. Uhlhorn and Bradley W. Klotz from NOAA's Hurricane Research Division. We thank Tomislava Vukicevic for her helpful discussions and Eric Uhlhorn for his comments and suggestions that greatly improved this manuscript. This research was made possible in part by a grant from BP/The Gulf of Mexico Research Initiative and a research grant from NASA (NNX14AM78G).

The Editor thanks Eric Uhlhon for his assistance in evaluating this paper.

References

Berner, J., G. J. Shutts, M. Leutbecher, and T. N. Palmer (2009), A spectral stochastic kinetic energy backscatter scheme and its impact on flow-dependent predictability in the ECMWF ensemble prediction system, *J. Atmos. Sci.*, *66*(3), 603–626, doi:10.1175/2008JAS2677.1.

Berner, J., S.-Y. Ha, J. P. Hacker, A. Fournier, and C. Snyder (2011), Model uncertainty in a mesoscale ensemble prediction system: Stochastic versus multiphysics representations, *Mon. Weather Rev.*, *139*(6), 1972–1995, doi:10.1175/2010MWR3595.1.

Cai, D., R. Kleeman, and A. Majda (2002), A mathematical framework for quantifying predictability through relative entropy, *Methods Appl. Anal.*, *9*(3), 425–444, doi:10.4310/MAA.2002.v9.n3.a8.

Davis, C., et al. (2008), Prediction of landfalling hurricanes with the Advanced Hurricane WRF model, *Mon. Weather Rev.*, *136*(6), 1990–2005, doi:10.1175/2007MWR2085.1.

Delnore, V., G. Bahn, W. Grantham, R. Harrington, and W. Jones (1984), Performance of airborne microwave remote sensors in Hurricane Allen, in *OCEANS 1984*, pp. 138–143, IEEE, Washington, D. C.

DelSole, T. (2004), Predictability and information theory: Part I. Measures of predictability, *J. Atmos. Sci.*, *61*(20), 2425–2440, doi:10.1175/1520-0469(2004)061<2425:PAITPI>2.0.CO;2.

DelSole, T., and M. K. Tippett (2007), Predictability: Recent insights from information theory, *Rev. Geophys.*, *45*, RG4002, doi:10.1029/2006RG000202.

Giannakis, D., and A. J. Majda (2012), Quantifying the predictive skill in long-range forecasting: Part II. Model error in coarse-grained Markov models with application to ocean-circulation regimes, *J. Clim.*, *25*(6), 1814–1826, doi:10.1175/JCLI-D-11-00110.1.

Judt, F., and S. S. Chen (2014), Rapid intensification in tropical cyclones: Understanding physical processes and forecast uncertainly using high-resolution stochastic ensembles, paper presented at 31st Conference on Hurricanes and Tropical Meteorology, Am. Meteorol. Soc., San Diego, Calif.

Judt, F., et al. (2015), Predictability of tropical cyclone intensity: Scale-dependent forecast error growth in high-resolution stochastic kinetic-energy backscatter ensembles, *Q. J. R. Meteorol. Soc.*, in press.

Kleeman, R. (2002), Measuring dynamical prediction utility using relative entropy, *J. Atmos. Sci.*, *59*, 2057–2072, doi:10.1175/1520-0469(2002)059<2057:MDPUUR>2.0.CO;2.

Klotz, B. W., and E. W. Uhlhorn (2014), Improved stepped frequency microwave radiometer tropical cyclone surface winds in heavy precipitation, *J. Atmos. Oceanic Technol.*, *31*(11), 2392–2408, doi:10.1175/JTECH-D-14-00028.1.

Komaromi, W. A., and S. J. Majumdar (2014), Ensemble-based error and predictability metrics associated with tropical cyclogenesis: Part I. Basinwide perspective, *Mon. Weather Rev.*, *142*(8), 2879–2898, doi:10.1175/MWR-D-13-00370.1.

Landsea, C. W., and J. L. Franklin (2013), Atlantic hurricane database uncertainty and presentation of a new database format, *Mon. Weather Rev.*, *141*(10), 3576–3592, doi:10.1175/MWR-D-12-00254.1.

Schenkel, B. A., and R. E. Hart (2012), An examination of tropical cyclone position, intensity, and intensity life cycle within atmospheric reanalysis datasets, *J. Clim.*, *25*(10), 3453–3475, doi:10.1175/2011JCLI4208.1.

Schneider, T., and S. M. Griffies (1999), A conceptual framework for predictability studies, *J. Clim.*, *12*(10), 3133–3155, doi:10.1175/1520-0442(1999)012<3133:ACFFPS>2.0.CO;2.

Shutts, G. (2005), A kinetic energy backscatter algorithm for use in ensemble prediction systems, *Q. J. R. Meteorol. Soc.*, *131*(612), 3079–3102, doi:10.1256/qj.04.106.

Uhlhorn, E. W., and P. G. Black (2003), Verification of remotely sensed sea surface winds in hurricanes, *J. Atmos. Oceanic Technol.*, *20*, 99–116, doi:10.1175/1520-0426(2003)020<0099:VORSSS>2.0.CO;2.

Uhlhorn, E. W., P. G. Black, J. L. Franklin, M. Goodberlet, J. Carswell, and A. S. Goldstein (2007), Hurricane surface wind measurements from an operational stepped frequency microwave radiometer, *Mon. Weather Rev.*, *135*(9), 3070–3085, doi:10.1175/MWR3454.1.

Uhlhorn, E. W., B. W. Klotz, T. Vukicevic, P. D. Reasor, and R. F. Rogers (2014), Observed hurricane wind speed asymmetries and relationships to motion and environmental shear, *Mon. Weather Rev.*, *142*(3), 1290–1311, doi:10.1175/MWR-D-13-00249.1.

Vukicevic, T., E. Uhlhorn, P. Reasor, and B. Klotz (2014), A novel multiscale intensity metric for evaluation of tropical cyclone intensity forecasts, *J. Atmos. Sci.*, *71*(4), 1292–1304, doi:10.1175/JAS-D-13-0153.1.

Yuter, S. E., and R. A. Houze (1995), Three-dimensional kinematic and microphysical evolution of Florida cumulonimbus: Part II. Frequency distributions of vertical velocity, reflectivity, and differential reflectivity, *Mon. Weather Rev.*, *123*, 1941–1963, doi:10.1175/1520-0493(1995)123<1941:TDKAME>2.0.CO;2.

Erratum

In the originally published version of this article, the acknowledgments contained a typographical error. The error has since been corrected, and this version may be considered the authoritative version of record.